Emission of acoustic phonons due to spin-flip electron transitions in nonsymmetric quantum wells

F. T. Vasko

Institute of Semiconductor Physics, National Academy of Sciences, pr. Nauki 45, Kiev, 252650, Ukraine
and Department of Electrical and Computer Engineering, Wayne State University, Detroit, Michigan 48202

V. V. Mitin

Department of Electrical and Computer Engineering, Wayne State University, Detroit, Michigan 48202

We have considered the emission of nonequilibrium acoustic phonons in the process of spin-flip transitions of electrons in nonsymmetric quantum wells. The spin splitting of the electron energy spectra causes the modifications of the energy and angular distributions as functions of the transverse voltage. The spin-flip contribution to the emission rate is substantial for the phonons being emitted at considerable angles to the normal direction. The intensity of phonon emission for such angles increases several times for InAs-based quantum wells, due to the contribution of spin-flip transitions.

Acoustic phonon emission by nonequilibrium two-dimensional electrons in different types of $Al_xGa_{1-x}As$-based heterostructures have been intensively investigated in the past two decades (see Ref. 1 and materials of recent conferences[2,3]). To the best of our knowledge, all these investigations dealt with spin-degenerate electron systems. At the same time, recent measurements of electron transport in the narrow-gap InAs-based[4,5] (and in the p-type GaAs-based[6]) nonsymmetrical heterostructures clearly show a spin-splitting energy of the order of a few meV, for heavily doped structures. This energy falls in the energy range of acoustic phonons ballistically propagating through the sample. Thus, the study of nonequilibrium phonon distributions (among other kinetic phenomena, e.g., spin-flip transitions under THz excitation[7] or spin-dependent tunneling[8]) provides an informative method for investigation of the electron-phonon interaction nonsymmetric narrow-gap quantum wells (QW's).

The peculiarities of phonon emission depend upon the spin splitting of the electron energy spectrum in the QW. As it is shown in Fig. 1, the electron dispersion law is determined not only by the two dimensional (2D) momentum $\mathbf{p}$ but also by the spin quantum number $\sigma = \pm 1$ in the following way: $\varepsilon_{\sigma p} = p^2/(2m) + \sigma v_s p$. Here σ is the spin projection onto the direction along $[\mathbf{p} \times \mathbf{v}_s]$ and the characteristic spin velocity $\mathbf{v}_s$ is along the normal to the 2D plane. This velocity is proportional to the applied transverse voltage and its numerical value is determined by the nonsymmetrical confined potential. Note that the dispersion law $\varepsilon_{\sigma p}$ is in-plane isotropic, because there is no distinguished direction in the 2D plane. Since the spin-split energy at the Fermi level $\varepsilon_s \equiv 2v_s p_F$ is equal to 3–4 meV for typical parameters of n-type InAs QW's (p_F is the Fermi momentum), the transitions between spin-split levels make a substantial contribution to the rate of acoustic-phonon emission under consideration. In this paper, we calculate the energy and angular distributions for the case of deformation electron-phonon interaction. The numerical estimations are done for the heavily doped QW's (with electron concentration of about 10^{12} cm^{-2}).

Based on the previous theoretical descriptions of acoustic phonon emission by 2D electrons[9,10] we express the differential energy flux as $\delta G \equiv \partial^2 G/(\partial\omega\partial\Omega)$, i.e., energy flux per unit solid angle, area, and frequency interval, through the rate of acoustic-phonon emission from nonsymmetrical QW, $I(\omega, \theta)$. This differential flux is written as

$$\delta G(\omega, \theta) = \frac{\partial^2 G}{\partial\omega\partial\Omega} = \frac{\hbar\omega^3}{(2\pi s)^3} I(\omega, \theta), \qquad (1)$$

where ω is an acoustic-phonon frequency, θ is a propagation angle with respect to the normal direction, and s is the longitudinal sound velocity. The rate of emission for a phonon with 3D wave vector $\mathbf{Q}$ in Eq. (1), $I_{\mathbf{Q}} \equiv I(\omega, \theta)$, is given by the general expression
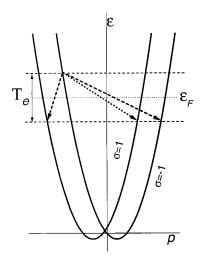

FIG. 1. The spin-split energy dispersion laws of electrons ($\sigma = \pm 1$ are the spin quantum numbers). Spin-flip and spin-conserving transitions are shown as dashed and dotted arrows, respectively.

     PRB **61**   11 047

$$I_{\mathbf{Q}} = \frac{2\pi}{\hbar} |C_Q|^2 \sum_{\alpha\beta} f_\alpha (1-f_\beta) |\langle \alpha| e^{-i\mathbf{Q}\cdot\mathbf{r}} |\beta\rangle|^2 \delta(\hbar\omega_Q - \varepsilon_\alpha + \varepsilon_\beta). \tag{2}$$

Here, the deformation interaction between the acoustic phonon with the linear dispersion law $\omega_Q = sQ$ and the electrons is described by the bulk matrix element $|C_Q|^2$ and the overlap factor $|\langle\alpha|\exp(-i\mathbf{Q}\cdot\mathbf{r})|\beta\rangle|^2$. The electron states in Eq. (2) are denoted by $|\alpha\rangle$, $|\beta\rangle$, with corresponding energies $\varepsilon_{\alpha,\beta}$ and distribution functions $f_{\alpha,\beta}$.

If only the lowest subband is occupied, and the parabolic approximation is valid for the electron dispersion law, the electron states in Eq. (2) take the form $|\alpha\rangle = |0\rangle|\sigma\mathbf{p}\rangle$ where $|0\rangle$ corresponds to the ground state of transverse motion and the spinor $|\sigma\mathbf{p}\rangle$ is determined by the eigenstate equation (see a more detailed description in Ref. 7):

$$\left\{ \frac{p^2}{2m} + \hat{\boldsymbol{\sigma}} \cdot [\mathbf{v}_s \times \mathbf{p}] \right\} |\sigma\mathbf{p}\rangle = \varepsilon_{\sigma p} |\sigma\mathbf{p}\rangle,$$

$$|\sigma\mathbf{p}\rangle = \frac{1}{\sqrt{2}} \left[1 + i \frac{(\hat{\boldsymbol{\sigma}} \cdot \mathbf{p})}{p} \right] |\sigma\rangle, \quad \sigma = \pm 1, \tag{3}$$

where m is the effective mass, $\hat{\boldsymbol{\sigma}}$ are the Pauli matrices, and $|\pm 1\rangle$ are the spin eigenvectors. Using Eq. (3), we transform the overlap factor in $I_{\mathbf{Q}}$ to the form

$$|\langle 0| e^{iq_\perp z} |0\rangle|^2 |\langle\sigma\mathbf{p}|\sigma'\mathbf{p}'\rangle|^2 \delta_{\mathbf{p},\mathbf{p}'+\hbar\mathbf{q}},$$

$$|\langle 0| e^{iq_\perp z} |0\rangle|^2 = \chi(q_\perp d)^2, \quad \chi(a) = \frac{(2/a)\sin(a/2)}{1-(a/2\pi)^2}. \tag{4}$$

The function $\chi(a)$ is written for the case of flat-band QW,[11] i.e., we suppose here that the drop of the potential across the QW is smaller than the energy of electron quantization in QW with the given width d, and the wave vector is written as $\mathbf{Q} = (\mathbf{q}, q_\perp)$. The spin-dependent matrix element $\langle\sigma\mathbf{p}|\sigma'\mathbf{p}'\rangle$ is expressed through the wave functions in Eq. (3) as follows:

$$\langle\sigma\mathbf{p}|\sigma'\mathbf{p}'\rangle = \frac{1}{2}$$
$$\times \begin{cases} 1 + \{(\mathbf{p}\cdot\mathbf{p}') + i\sigma[\mathbf{p}\times\mathbf{p}']_z\}/(pp'), & \sigma = \sigma' \\ i\langle\sigma|\hat{\boldsymbol{\sigma}}|\sigma'\rangle \cdot (\mathbf{p}'/p' - \mathbf{p}/p), & \sigma \neq \sigma'. \end{cases} \tag{5}$$

After simple transformations of Eq. (5) we obtain

$$|\langle\sigma\mathbf{p}|\sigma'\mathbf{p}'\rangle|^2 = \frac{1}{2} \times \begin{cases} 1 + \cos(\widehat{\mathbf{p},\mathbf{p}'}), & \sigma = \sigma' \\ 1 - \cos(\widehat{\mathbf{p},\mathbf{p}'}), & \sigma \neq \sigma', \end{cases} \tag{6}$$

so that the spin-flip transitions are forbidden in the case of zero momentum transfer ($\mathbf{p} = \mathbf{p}'$).

Thus, the general expression (2) for the rate of phonon emission is transformed into

$$I(\omega,\theta) = \frac{\hbar\bar{\nu}}{4p_F} \frac{\hbar\omega}{sv_F} \chi(q_\perp d)^2 \sum_{\sigma\sigma'} \int \frac{d\mathbf{p}}{(2\pi\hbar)^2} f_{\sigma\mathbf{p}+\hbar\mathbf{p}/2}$$
$$\times (1 - f_{\sigma'\mathbf{p}-\hbar\mathbf{q}/2}) |\langle\sigma\mathbf{p}+\hbar\mathbf{p}/2|\sigma'\mathbf{p}-\hbar\mathbf{q}/2\rangle|^2$$
$$\times \delta(\hbar\omega_Q - \varepsilon_{\sigma\mathbf{p}+\hbar\mathbf{p}/2} + \varepsilon_{\sigma'\mathbf{p}-\hbar\mathbf{q}/2}). \tag{7}$$

Here, we introduced the characteristic relaxation rate $\bar{\nu} = (Dp_F)^2 m/(\pi\hbar^4\rho s)$, $v_F = p_F/m$ is the Fermi velocity, D is the deformation potential, and ρ is the density of the heterostructure. Elastic properties of the heterostructure are supposed to be uniform. In the following we neglect a small in-plane anisotropy of electron distribution function and suppose that $f(\varepsilon_{\sigma p})$ is the quasiequilibrium distribution function with the electron temperature T_e and the Fermi energy ε_F. In order to perform the angle integration in Eq. (7), we use the δ function taking into account that only small $\cos(\widehat{\mathbf{p},\mathbf{p}'})$ are essential, if $\sin\theta \gg s/v_F$. Upon this integration, we obtain the differential energy flux in the form

$$\delta G(\omega,\theta) \simeq \overline{\delta G} \left(\frac{\hbar\omega}{sp_F} \right)^3 \frac{\chi(q_\perp d)^2}{2p_F \sin\theta} \frac{\varepsilon_F}{T_e} \sum_\sigma \int_0^\infty$$
$$\times dp \left\{ \frac{2p^2}{p(q)^2} f\left(\varepsilon_{\sigma p(q)} + \frac{\hbar\omega}{2} \right) \left[1 - f\left(\varepsilon_{\sigma p(q)} - \frac{\hbar\omega}{2} \right) \right] + \frac{(\hbar q)^2}{p(q)^2} f\left(\varepsilon_{-\sigma p(q)} + \sigma v_s p(q) + \frac{\hbar\omega}{2} \right) \right.$$
$$\left. \times \left[1 - f\left(\varepsilon_{-\sigma p(q)} - \sigma v_s p(q) - \frac{\hbar\omega}{2} \right) \right] \right\} \tag{8}$$

and the second term in Eq. (8) describes the contribution of spin-flip transitions. We use here the notation $p(q) \equiv \sqrt{p^2 + (\hbar q/2)^2}$ and the characteristic energy flux $\overline{\delta G}$ is determined as

$$\overline{\delta G} = \frac{\hbar\bar{\nu}sv_F}{(2\pi)^3\hbar^2}. \tag{9}$$

The main contributions to the integral in formula (8) come from the momentums of the order of p_F, and an exponential cutoff of $\delta G(\omega,\theta)$ takes place under the condition $\hbar q/p_F > 1$, i.e., we again suppose that θ is not small. Further analytical simplifications are based on the inequality $T_e/\varepsilon_F \ll 1$, which allows us to replace the exponential drop of δG by the step function and to obtain

$$\frac{\delta G(\omega,\theta)}{\overline{\delta G}} \simeq t\Omega^3 \chi(q_\perp d)^2 \frac{\theta[1-(\Omega\sin\theta/2)^2]}{\sqrt{1-(\Omega\sin\theta/2)^2}}$$
$$\times \left\{ \frac{\Omega/t}{\sin\theta(e^{\Omega/t}-1)} + \left(\frac{\Omega}{2}\right)^2 \sin\theta \left(\frac{1}{2} \left[\frac{(\Omega-1)/t}{e^{(\Omega-\gamma)/t}-1} \right. \right. \right.$$
$$\left. \left. \left. + \frac{(\Omega+\gamma)/t}{e^{(\Omega+1)/t}-1} \right] - \frac{\Omega/t}{e^{\Omega/t}-1} \right) \right\}, \tag{10}$$

where $q_\perp d = \Omega(p_F d/\hbar)\cos\theta$. We have also introduced in Eq. (10) the dimensionless frequency $\Omega = \hbar\omega/sp_F$, temperature $t = T_e/sp_F$, and parameter $\gamma = v_s/s$.
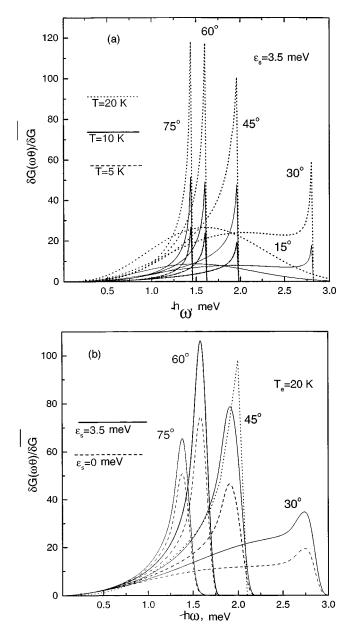
FIG. 2. The differential acoustic flux (in units $\overline{\delta G}$) versus phonon energy $\hbar\omega$ for the different propagation angles and electron temperatures (a), and for different propagation angles and spin-splitting energies (b).

The numerical calculations have been performed for the InAs-based QW with the width 10 nm and spin-splitting energy ε_s varied from zero (symmetric QW) to 3.5 meV, in agreement with the experimental data.[4,5] The energy distribution of the emitted phonons for different angles of propagation is plotted in the units $\overline{\delta G} \simeq 0.7 \times 10^{-16}$ J/cm^2 sr in Fig. 2. Since the spin-flip matrix element is vanished for the small-momentum transfer case, which corresponds to the small-angle region, we do not consider here $\theta < 15°$, where $\delta G(\omega, \theta)$ increases substantially (see discussion in Ref. 10). Figure 2(a) shows the energy dependencies of δG calculated by the simplified formula (10) for the maximal spin-splitting energy, at different temperatures. The phonon emission has a threshold at the cutoff energy $2sp_F/\sin\theta$ for the not-small-angle region (see Ref. 12) and δG increases as the inverse square root at threshold if $T_e/\varepsilon_F \ll 1$. These results demon-
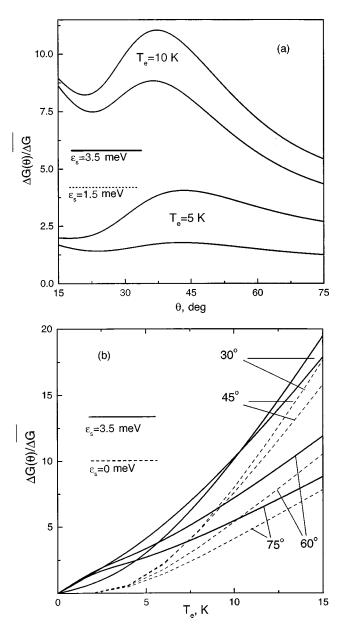
FIG. 3. The emission intensity (in units $\overline{\Delta G}$) as function of propagation angle, for different T_e and ε_s (a) and as function of electron temperature for different θ (b).

strate strong temperature dependencies of near-threshold peaks. More accurate calculations based on Eq. (8) show the smearing of the thresholds, but the dependence of the cutoff energy on spin-splitting energy is weak, because $v_s \ll v_F$ [see Fig. 2(b)]. Nevertheless, the maximum value of δG is substantially increased in the threshold region (up to two times for $\theta = 45°$ if ε_F is varied from 0 to 3.5 meV). Note also, that Eq. (10) overestimates the peak values of δG, compared to Eq. (8), as shown by an additional dotted line for $\theta = 45°$ in Fig. 2(b).

The emission intensity is introduced by $\Delta G(\theta) = \int_0^\infty d\omega\, \delta G(\omega, \theta)$, and simple numerical integration of Eq. (10) [or Eq. (8)] provides us with the angular dependence of $\Delta G(\theta)$. The plots of ΔG versus θ for different ε_s and T_e and ΔG versus T_e for different θ and T_e are presented in Figs. 3(a) and 3(b), respectively. The characteristic intensity $\overline{\Delta G}$ is equal to 0.16 mW/cm^2 sr for the above used param-

eters. The angle dependencies of the emission intensity demonstrate the sharp increase for the small-angle region and ΔG vanishing as $\theta \to \pi/2$. Besides, the $\Delta G(\theta)$ drops in the region around $20°$ [see Fig. 3(a)], where the transition occurs from the hump-type energy distribution [curves for $\theta = 15°$ in Fig. 2(a)] to the threshold-type curves. The spin-flip-transition contributions are most essential in the region of intermediate angles $[\pi/4-\pi/3]$, where ΔG increases with both the spin-splitting energy and the electron temperature. The variation of ΔG with ε_s is substantial (up to several times) for low temperatures, while for the region $T_e > 10$ K the emission intensity increases only by $10-30\%$. The contribution of spin-flip transitions is greater for the lower doping levels, when the ratio v_s/v_F increases. Thus, the low-doped structures are more promising for studying spin-flip transitions.

In conclusion, we have studied the new channel of phonon emission due to spin-flip transitions of electrons in the nonsymmetric narrow-gap quantum wells. Our considerations were based on the parabolic model of 2D electronic states (the nonparabolic corrections to $\varepsilon_{\sigma p}$ and to electron-

phonon matrix element are of the order of $\varepsilon_F/\varepsilon_g \ll 1$; ε_g is the band-gap energy) and on temperature approximation for nonequilibrium electron distribution.[13] We also neglected the near-surface modifications of the phonon modes; according to recent calculations of electron relaxation rates,[14] this effect is not essential if the top cladding layer width is bigger than d. We have obtained substantial modification of the energy and angular distributions of the emitted phonons due to spin-flip contribution for the angles far from the normal direction. Thus this new channel of phonon emission can be studied experimentally by direct measurements. In addition the investigation of nonequilibrium spin distribution of electrons becomes possible, due to considerable variation of the matrix element (6). More sensitive measurements of phonon emission can be possible in a quantized magnetic field, where the peculiarities of spin-split Landau level should be essential. It is also interesting to examine the phonon emission by photoexcited carriers with the energies near the extrema of spin-split bands.

[1] L. J. Challis, in *The Physics of Low-Dimensional Semiconductor Structures*, edited by Butcher, N. H. March, and M. P. Tosi (Plenum Press, New York, 1993).

[2] Proceedings of the International Conference on Phonons'95, edited by T. Nakayama, S. Tamura, and T. Yagi [Physica B **219 & 220**, (1996)].

[3] Proceedings of the International Conference on Phonons'98, edited by M. Giltow, A. Kozorezov, and K. Wigmore [Physica B **263 & 264** (1999)].

[4] J. P. Heida, B. J. van Wees, J. J. Kuipers, T. M. Klapwijk, and G. Borghs, Phys. Rev. B **57**, 11 911 (1998).

[5] J. Nitta, T. Akazaki, H. Takayanagi, and T. Enoki, Phys. Rev. Lett. **78**, 1335 (1997).

[6] S. J. Papadakis, E. P. De Poortere, H. C. Manoharan, M. Shayegan, and R. Winkler, Science **283**, 2056 (1999).

[7] F. T. Vasko and O. Keller, Phys. Rev. B **58**, 15 666 (1998).

[8] A. Voskoboynikov, S. S. Liu, and P. C. Lee, Phys. Rev. B **59**, 12 514 (1999).

[9] F. T. Vasko, O. G. Balev, and P. Vasilopoulos, Phys. Rev. B **47**, 16 433 (1993); F. T. Vasko, Fiz. Tverd. Tela (Leningrad) **30**, 2092 (1988) [Sov. Phys. Solid State **30**, 1207 (1988)].

[10] V. V. Mitin, G. Paulavicius, N. A. Bannov, and M. A. Strocio, J. Appl. Phys. **79**, 8955 (1996).

[11] P. J. Price, Ann. Phys. (N.Y.) **133**, 217 (1981).

[12] V. F. Gantmakher and I. B. Levinson, *Carrier Scattering in Metals and Semiconductors* (Elsevier Science, Amsterdam, 1987).

[13] A more complicated character of emission is expected in the case of nonequilibrium spin distribution of the electrons (which can be easily realized, because the spin relaxation is more slow than energy and momentum relaxation). Another complication of the phonon emission can be caused by strong in-plane anisotropy of the electron distribution (cf. consideration Ref. 10 for the spin-degenerate case).

[14] V. I. Pipa, F. T. Vasko, and V. V. Mitin, J. Appl. Phys. **85**, 2754 (1999).